

PERFORMANCE OPTIMIZATION OF A CONVERGENT-DIVERGENT DUCT USING DAKOTA ENVIRONMENT

PhD candidate: **Andrea Ottonello** (badge number: 3697081)

DIME - University of Genoa, Via Montallegro 1,
16145 Genova (GE) - ITALY

ABSTRACT

The aim of this project is the performance optimization of a fixed geometry nozzle by working on its inlet boundary conditions. Considering a real case, a convergent-divergent duct is designed through formulas and tables of gas dynamics in a certain steady-state condition. If the transient behavior of the component is characterized by strong off-design of inlet conditions, it can be useful to identify possible combinations of the input thermodynamic quantities capable to maximize nozzle performance out of design point (e.g. to obtain the maximum outlet speed and minimum total pressure drop through the component).

The numerical analyses have been performed using ANSYS Fluent, which has been 'fork' interfaced with Dakota optimizer. In order to speed up the simulations necessary for the generation of the database and considering that the duct is axial-symmetric, a 2D grid has been developed in ICEM CFD.

The first phase of the project consists in a DoE inside duct operating field, aimed at the generation of response surfaces. These ones have been used in a second phase for the development of a surrogate model, on which a multi-objective genetic optimization algorithm has been applied.

NOMENCLATURE

p	pressure [N/m ²]
r	radius [mm]
A	cross section [mm ²]
D	diameter [mm]
L	length [mm]

M	mach number
R	characteristic expansion ratio static to total
T	temperature [K]
V	velocity [m/s]

Subscripts

1	convergent inlet
2	divergent outlet
I	unitary mach number condition in at least one nozzle section
III	supersonic condition with isentropic expansion in the divergent
g	throat section
in	nozzle inlet
out	nozzle outlet
s	discharge
t	total
u	nozzle outlet
x	axial direction

Apex

*	critical condition (M=1)
---	--------------------------

Acronymics

delta	differential (inlet-outlet nozzle)
DoE	Design of experiments
EA	Evolutionary algorithm
GA	Genetic algorithm
MOGA	Multi-objective genetic algorithm

1. INTRODUCTION AND FORMULATION OF THE PROBLEM

1.1 Convergent-divergent project at design point

Nozzle design follows some simple formulas of gas dynamics that link the total conditions to the static ones, allowing to determine the “critical” state (unitary Mach) starting from convergent inlet boundary conditions. Once assigned fluid properties, target mass flow rate and total inlet conditions (see Table 1), the “throat” diameter of the duct is constrained (D_g in Table 2). The diameter D_1 (convergent inlet section - Figure 1) defines instead the Mach number at the inlet section from total upstream conditions and the mass flow equation.

In general the outlet diameter of the divergent (D_2) is a free parameter capable of heavily conditioning outlet flow conditions. For the case under examination it is assumed that the outlet pressure of the divergent ($p_u = p_2$) is fixed and the diameter D_2 is locked by design constraints. Assuming isentropic flow from the entrance to the exit of the nozzle (ideal case), the A_u/A_g ratio corresponds in the compressible flows tables to two different solutions (one

subsonic and another one supersonic [1, 2]) or to two different values of the p_s/p_{t1} ratio; in the supersonic solution, as known, we have $p_s/p_{t1} = R_{III}$.

In our case the outlet static pressure of the divergent (p_u) is imposed equal to the discharge pressure (p_s). Therefore if the ratio p_2/p_{t1} actually available is higher than the one taken from compressible flows table (R_{III}) [2], but in any case lower than the value strictly necessary to obtain $M_g = 1$ and subsonic flow in the rest of the duct ($R_I = p^*/p_{t1}$), the nozzle will be characterized by a shock wave in a section of the divergent preceding the outlet, causing total pressure losses and a substantial reduction in jet speed [1, 2].

Considering the abovementioned design constraints, in this optimization problem we want to work onto inlet total conditions in order to optimize the convergent-divergent performance, i.e. to obtain the maximum nozzle outlet flow speed and minimum total pressure drop through the static component.

Boundary conditions						
Inlet tot pressure (pt1) [Pa]	Inlet tot temperature (Tt1) [K]	target mass flow [kg/s]	Outlet static pressure (p2) [Pa]	$p^*/pt1$	$p2/pt1$	R_{III}
500000	400	0.600	120000	0.528	0.240	0.085

Design choices				
Convergent inlet diameter (D1) [mm]	Throat diameter (Dg) [mm]	Divergent outlet diameter (D2) [mm]	Convergent length (L1) [mm]	Divergent length (L2) [mm]
34.67	27.50	40.00	200.00	400.00

Tables 1 & 2 : BCs assigned to nozzle design (upper table) and design choices (lower table)

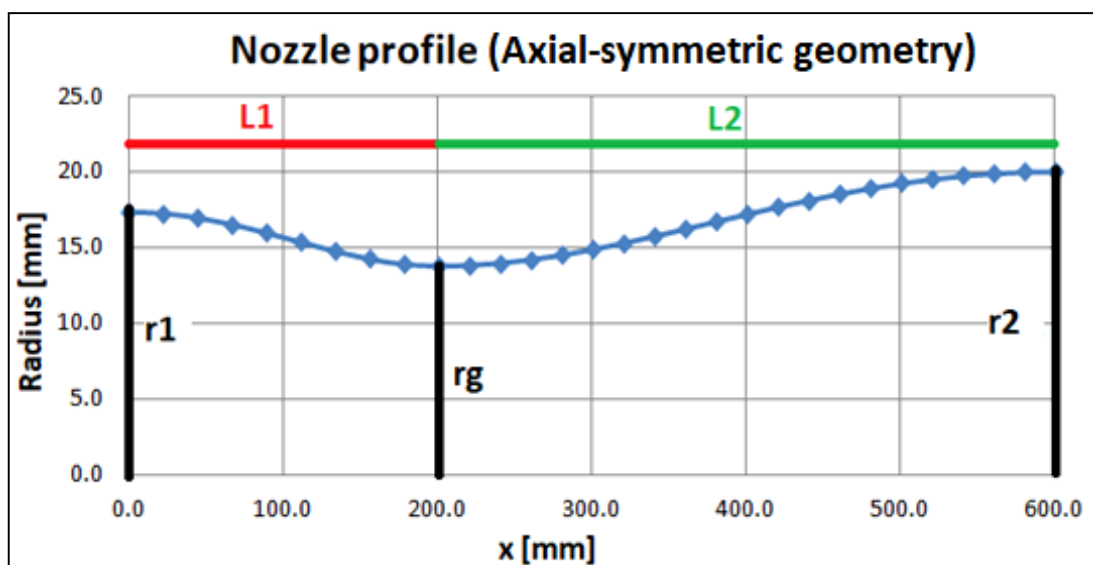


Figure 1 : nozzle 2D profile, generated by points. The fundamental geometric quantities are quoted

1.2 Mesh details

As mentioned above, given the duct axial-symmetric nature, a two-dimensional mesh of half geometry has been generated. The calculation grid used is structured and created using the blocking technique in the ICEM CFD environment. In order to solve the boundary layer on the viscous walls of the duct, a bi-geometric law was used for the generations of the cells, differentiating the expansion ratio used for the region close to the axis of symmetry (the "core flow region", where there are no wall effects but only viscous effects between fluid particles) from that one used for the duct outline, where the prism layer [3] is required to obtain an accurate resolution of the boundary layer, essential for an effective estimation of nozzle crossing losses (which represent one of the two objective functions of the optimization) .

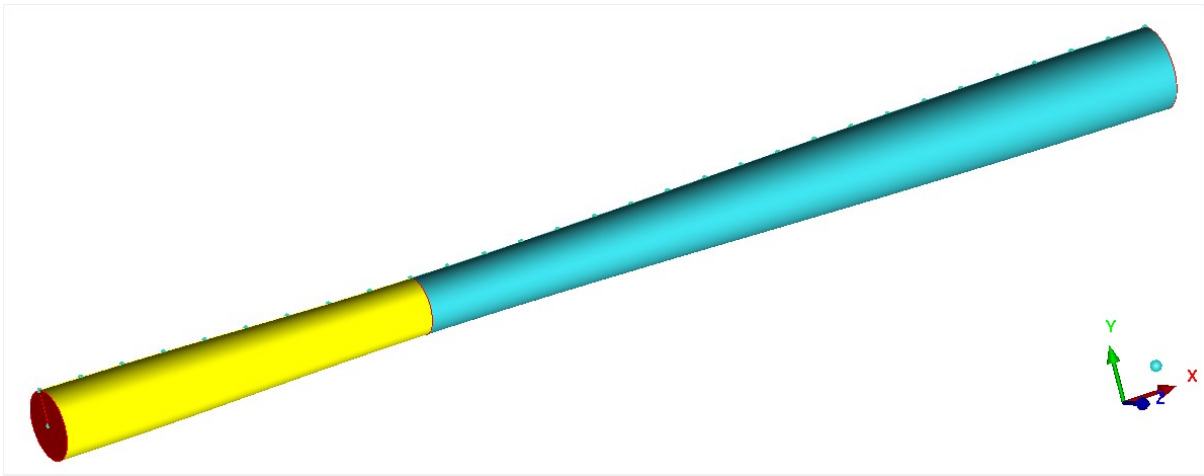


Figure 2 : nozzle 3D geometry, obtained by surface of revolution from the 2D profile of the duct extrapolated by points (convergent duct in yellow and divergent in blue)

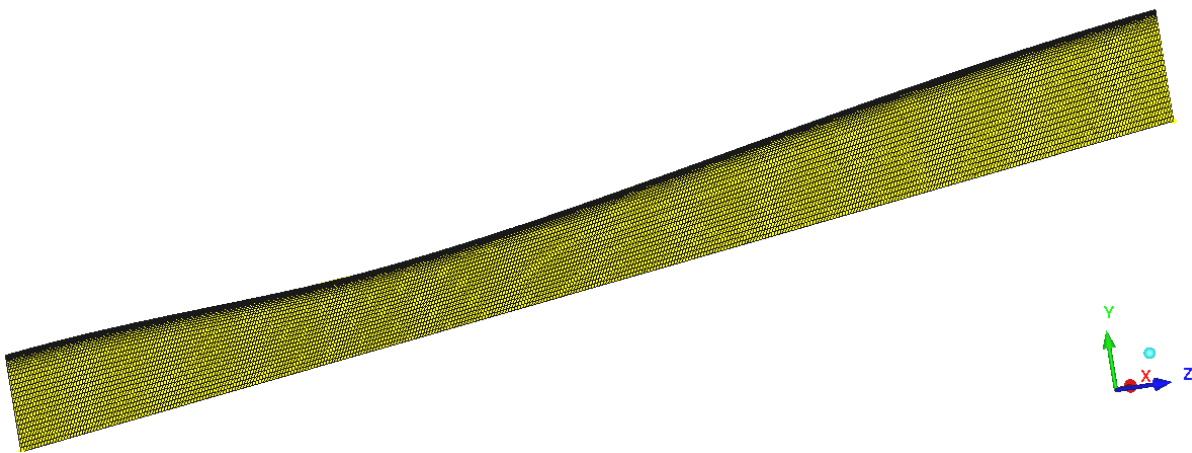


Figure 3 : side view of halved nozzle 2D mesh (27000 cells). It is possible to notice the condensation of elements operated on the outline (wall condition)

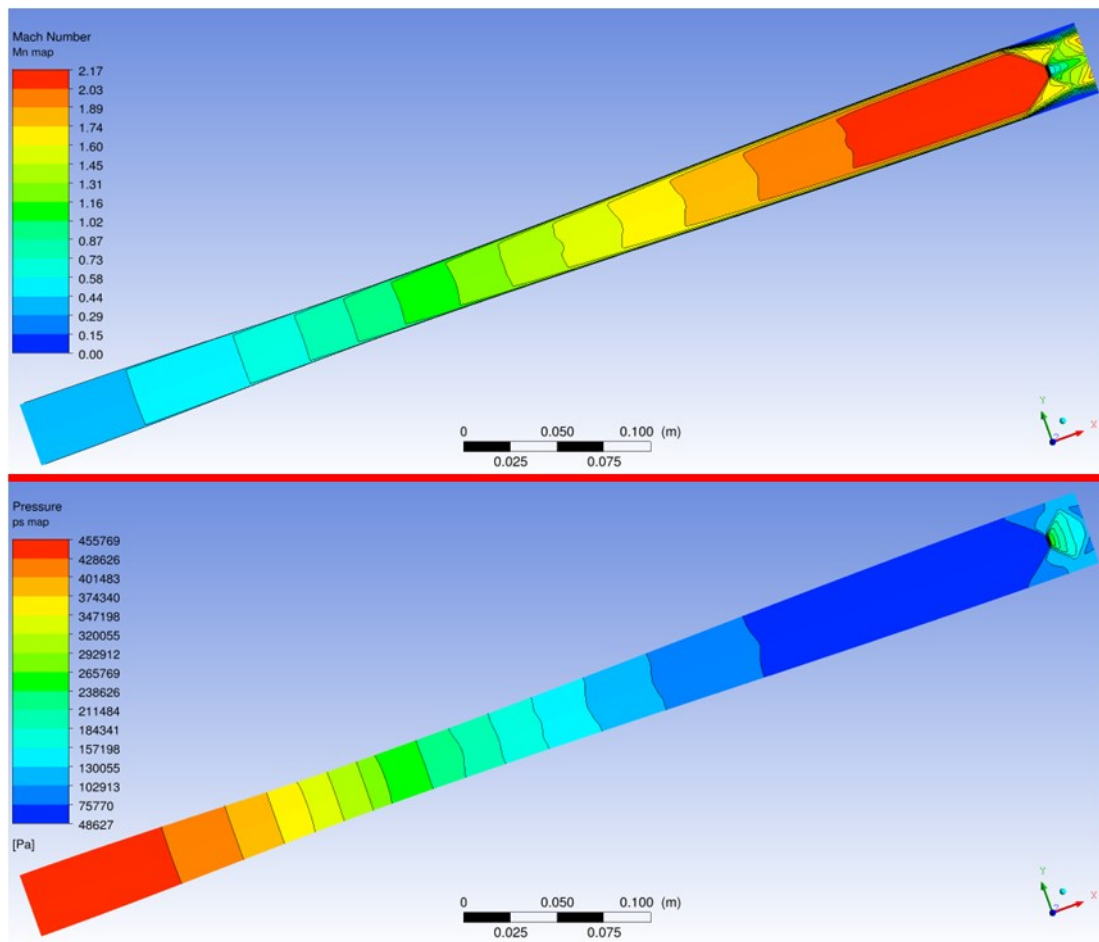
1.3 Design point simulation

The phase following grid generation consists in importing the mesh into the pre-processor and solver (Fluent). In addition to the use of energy equation, a k-omega numerical turbulence model [3] has been adopted; Shear Stress Transport (SST) turbulence closure

make possible to predict accurately the trigger and the degree of flow separation. The simulation has been set up as axial-symmetric, convergent inlet has been set as ‘pressure-inlet’ to which p_{t1} and T_{t1} have been assigned, while divergent outlet has been simulated as ‘pressure-outlet’ to which the discharge pressure $p_2 = 120$ [kPa] have been attributed.

The setting of the code to reach calculation convergence has proved rather complex, making necessary the use of more than one type of solver. Each simulation required about a thousand iterations to achieve convergence.

Post-processing images of the calculation performed at the design point confirm that nozzle behavior falls between ‘ R_I ’ and ‘ R_{III} ’ states with shock wave located in the divergent just before the outlet section. The shock wave causes a considerable drop in divergent outlet flow speed as also evidenced by the localized increase in static pressure downstream of the wave.



Figures 4 & 5 : Mach Number (upper figure) and static pressure (lower figure) contours at design point

Results @ design point			
Inlet total temperature (T_{t1}) [K]	Inlet total pressure (p_{t1}) [Pa]	Divergent outlet velocity [m/s]	Total pressure drop across the nozzle [Pa]
400	500000	481.1	94999.7

Table 3 : results summary at design point

2. DOE GENERATION

2.1 Multidimensional parameter study

As a first step towards nozzle performance optimization, a DoE was implemented; in this first case in the form of a multidimensional (2 dimensions) parameter study on the input variables (p_{t1} and T_{t1}). In particular the design space has been divided through a regular grid of 10 intervals for each parameter, which leads to a total of 121 simulations. The target is to evaluate the dependency of the objective functions from input variables, so as to exploit this information in the subsequent optimization phase (paragraph 3).

Considering to vary the inlet total pressure in a range of +/- 1 [bar] with respect to the design condition (5 [bar]) and the total temperature in a range of +/- 100 [K] with respect to the design (400 [K]), an acceptable resolution of 20 [kPa] is obtained for the first variable and of 20 [K] for the second one.

The multidimensional parameter study makes use of the '*single model*' which is characterized by a single interface instance to map variables into responses. Another important feature of Dakota input file '*dakota_nz_project_DOE.in*' is the adoption of a '*fork*' interface to put in communication the optimizer with an external solver; moreover, this type of interface is recommended when, as in the case in question, the calculations are performed asynchronously (two different simulations at a time – '*evaluation_concurrency*' = 2).

For each of the 121 input parameter combinations, the Fluent solver is "called" from the '*analysis_driver*', a bash script necessary to interface the simulation code to Dakota using a fork interface. The '*simulator_script*' file supplies pre- and post-processing functionality in order to transfer the input parameters from Dakota to Fluent and to extract the response values of interest from the simulator's output file for return to the optimizer [4].

At first the solver loads a base case ('*Project_geo_ref_case3.cas*' – pre-processing file, generated to simulate the design condition shown in paragraph 1.3) inserted in '*templatedir*' (a directory containing the template case for each simulation). Then Fluent executes the instructions contained in a journal file ('*Fluent_auto.jou*' consists of a series of instructions compatible with the Fluent command line) which provide for:

- the setting of the boundary conditions (taken from '*params.in*' file);
- the definition of the monitors of the thermo-fluid dynamic quantities in various control section (inlet, throat and outlet) in '*.out*' format;
- the setup of the computational models used by the solver.

Finally the flow speed at divergent outlet and the total pressure drop through the nozzle, i.e. the two objective functions, have been extrapolated through post-processing instructions developed in the '*simulator_script*' file and inserted alongside the values of the input BCs on each row of the output results table ('*table_out.dat*').

DoE results can then be plotted through a program suitable for the elaboration of numerical data (e.g. Scilab): the visualization of the 3D surfaces obtained by linear interpolation on the database allows to evaluate the sensitivity of the objective functions to the input variables and

to analyze the behavior of these functions, appropriately directing the choice of the optimization algorithm to be used in the next phase.

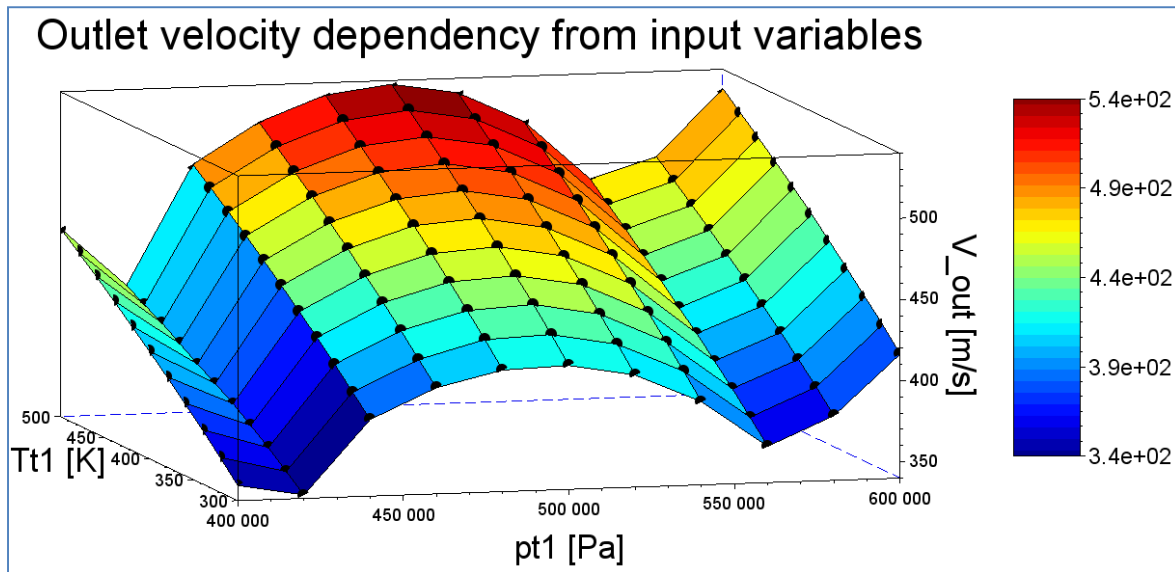


Figure 6 : multidimensional parameter study on divergent outlet flow speed (Scilab surface plot with contour map). Black dots on the surface represent the sample sites

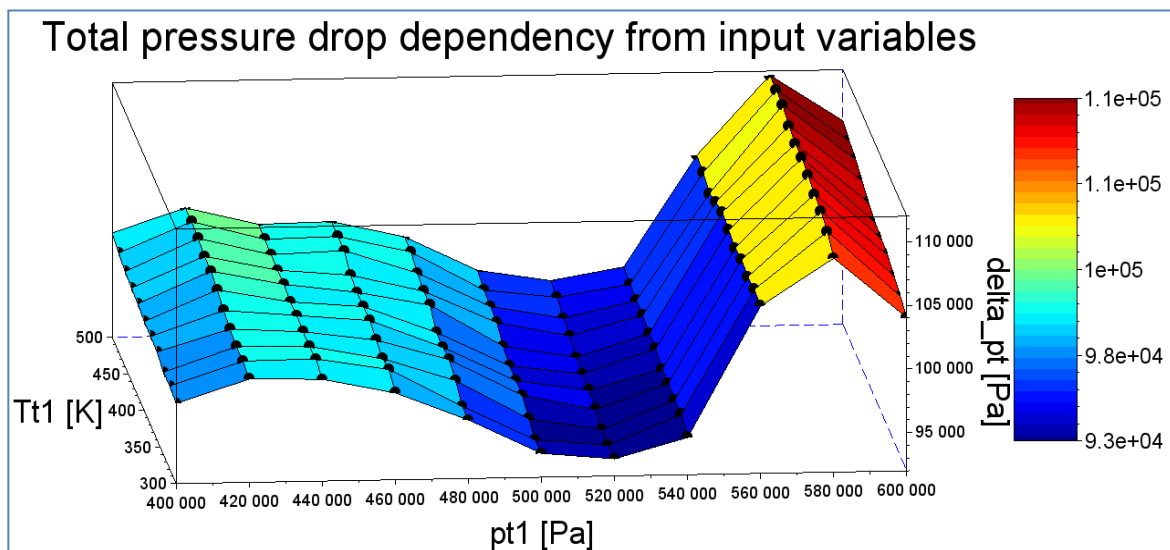


Figure 7 : multidimensional parameter study on total pressure drop through the nozzle (Scilab surface plot with contour map).

2.2 Latin Hypercube Sampling

In addition to the parameter study shown above, it was decided to generate another DoE, but in this case adopting a ‘space-filling’ technique. Methods like *Latin Hypercube Sampling* generally behave better for building a metamodel in case of irregular responses like that ones shown in figures 6 & 7.

In the examined case we have $k = 2$ input parameters and $N = 121$ samples; ‘*dace lhs*’ sampling method generate a sampling matrix $S_{N \times k}$ containing the samples in its rows [5]:

$$\bar{S} = \frac{1}{N} (\bar{Q} - \bar{R}) \quad (1)$$

where:

- $Q_{N \times k}$ is a matrix whose columns are random permutations of the integers from 1 to N;
- $R_{N \times k}$ is a matrix with random values uniformly distributed in [0,1].

Apart from the variation made on the 'method', the input file of Dakota 'dakota_nz_project_DOE_LHS.in' presents the same settings used before for the multidimensional parameter study (same objective functions, bounds to the input variables, etc.) and employs the same *analysis_driver*.

LHS results are shown in the images that follow and confirm the trends of the objective functions already seen in the multidimensional parameter study:

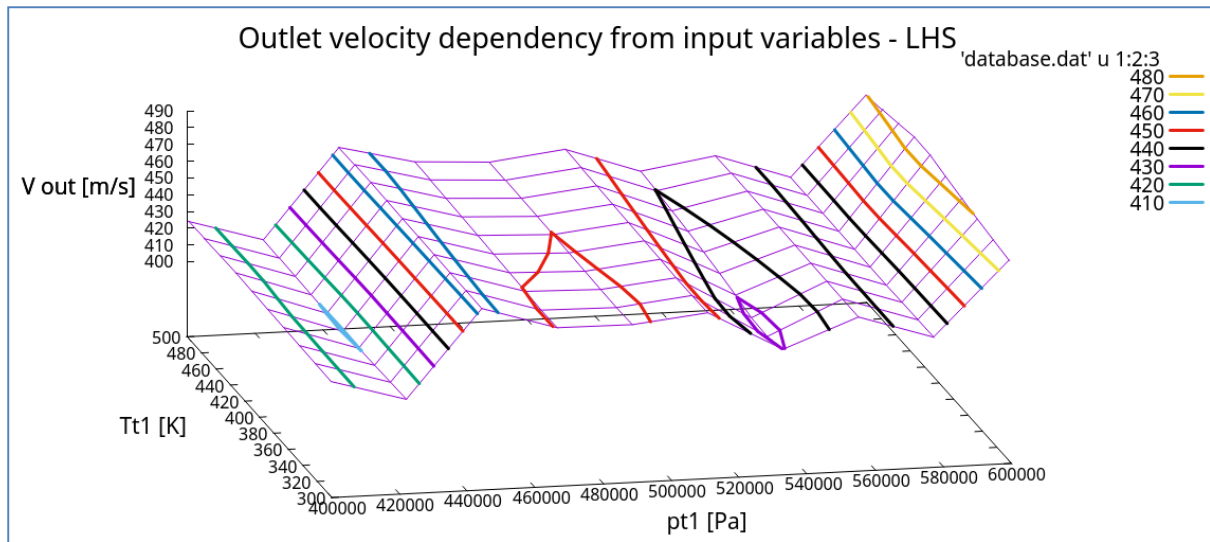


Figure 8 : divergent outlet flow speed surface grid with contour lines (Gnuplot), resulting from LHS

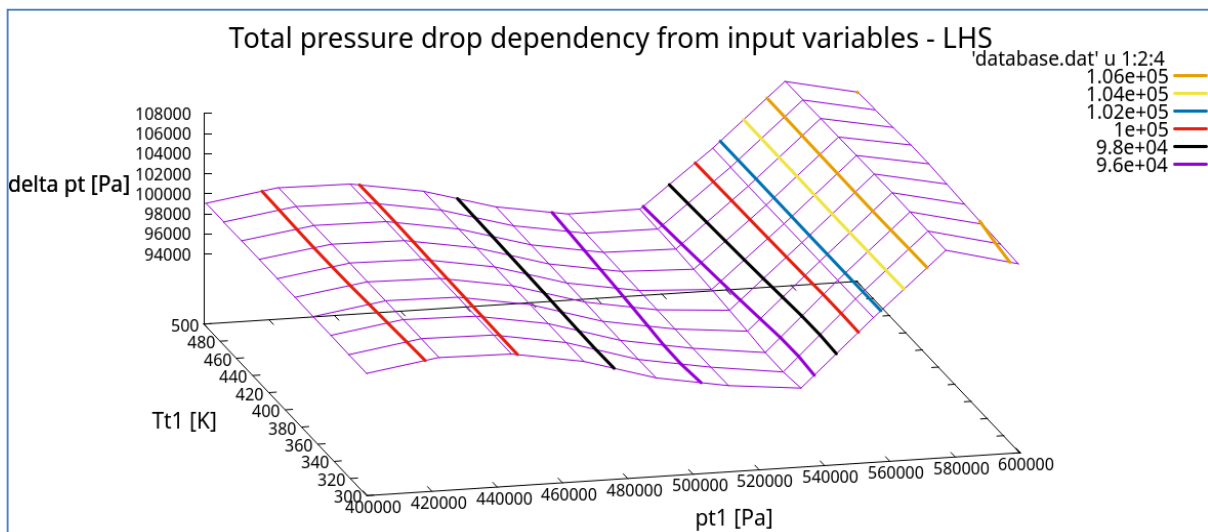


Figure 9 : total pressure drop surface grid with contour lines (Gnuplot), resulting from LHS

3. GENERATION OF RESPONSE SURFACES (*GAUSSIAN_SURFPACK*) AND MULTI-OBJECTIVE GENETIC OPTIMIZATION (*MOGA*)

The 3D surfaces extracted from the DoEs illustrated in the previous paragraph highlight the presence of local minima and maxima for the two objective functions inside the design space. This led to discard optimization methods based on the gradient, directing the choice toward an evolutionary algorithm, considered more robust for the case study.

At the beginning the genetic algorithm identifies a randomly selected population of design points in the parameter space (*initialization_type* = *unique_random*), where the values of the design parameters form a “genetic string” that uniquely represents each “individual” of the population. Then the EA give birth to a sequence of generations, where the best design points in the population (i.e. in this case those having minimum *delta p_t* and maximum *V_{out}*) are considered to be the most “fit” and are allowed to survive and reproduce.

It is possible to manage the way of generating new individuals through specific input file settings like *crossover_rate*, *mutation_rate*, *num_offspring*, *num_parents*, etc.

In this optimization problem there is more than one objective function, therefore it is necessary to apply a multi-objective algorithm. It must be remembered that optimal design in a multi-objective problem is usually a set of points called the Pareto front. Each point on the Pareto front satisfies the Pareto optimality criterion: *“a feasible vector X* is Pareto optimal if there exists no other feasible vector X which would improve some objective without causing a simultaneous worsening in at least one other objective”* [4, 6].

From this follows that if a feasible point X' exists that can be improved on one or more objectives simultaneously, it is not Pareto optimal: it is said to be *“dominated”* and the points along the Pareto front are said to be *“non-dominated”*.

The optimization developed in this project uses the *‘moga’* i.e. a multi-objective genetic algorithm based on the idea that as the population evolves in a GA, individuals that are “non-dominated” are chosen to remain in the population.

Entering into details, MOGA algorithm is characterized by two main 'operators' [4] called:

- ❖ *‘domination_count’* fitness assessor, which works by ranking population individuals such that the fitness level of an individual within a certain generation depends on how many other designs "dominate" the one in question;
- ❖ *‘below limit’* selector, which chooses individuals for next generations by discarding a design if dominated by more than a specified number of other ones. Otherwise the individual in question is kept and selected to go to the next generation.

That said, a minimum number of selections must take place for each generation and the *‘shrinkage_fraction’* represents the minimum percentage of the population size that must go on to the subsequent generation. So if the selector does not find a sufficient number of points to respect the constraint imposed by the aforesaid percentage, it relaxes its limit and makes selections from the remaining designs.

Another problem posed by the project in question is that input variables have orders of magnitude that are very different ($p_{t1} \approx 10^5$, $T_{t1} \approx 10^2$), as the objective functions ($\Delta p_t \approx 10^5$, $V_{out} \approx 10^2$). The search for ‘optimum’ designs can be conducted more efficiently by reducing the different quantities involved on a unitary scale (0-1); to do so, the ‘*scaling*’ keyword has been specified in the ‘*method*’ specification inside Dakota input file (*dakota_nz_project_sbo_moga_scaling.in*).

The disadvantage of genetic algorithms is, as well known, the computational cost; however this can be significantly amortized if, as in the project presented here, one opts for the use of a surrogate model (*‘surrogate global’*) of the physical problem in question.

The target of generating a meta-model is to produce an inexpensive approximate model that is intended to capture the salient features of an expensive high-fidelity model (i.e. the actual physical model, with which the DoE was generated).

In particular a “response surface method” (which involve many points spread over the parameter ranges of interest) has been used. This surface fitting method work in conjunction with the design of experiments previously described at paragraph 2.

The developed surrogate model implements the *‘gaussian process surfpack’* which uses the Gaussian correlation function with parameters that are selected by Maximum Likelihood Estimation (MLE); this correlation function results in a response surface that is C^∞ -continuous.

The Kriging (also known as Gaussian process - GP) method uses techniques developed in the geostatistics and spatial statistics communities to produce smooth surface fit models of the response values from a set of data points. The form of the GP model [4] is:

$$\hat{f}(\bar{x}) \approx \bar{g}(\bar{x})^T \bar{\beta} + \bar{r}(\bar{x})^T \bar{R}^{-1} (\bar{f} - \bar{G}\bar{\beta}) \quad (2)$$

where:

- \bar{x} is the current point in n-dimensional parameter space;
- $\bar{g}(\bar{x})$ is the vector of trend basis functions evaluated at \bar{x} ;
- $\bar{\beta}$ is a vector containing the generalized least squares estimates of the trend basis function coefficients;
- $\bar{r}(\bar{x})$ is the correlation vector of terms between \bar{x} and the data points;
- \bar{R} is the correlation matrix for all of the data points;
- \bar{f} is the vector of response values;
- \bar{G} is the matrix containing the trend basis functions evaluated at all data points.

The terms in the correlation vector and matrix are computed using a Gaussian correlation function and are dependent on an n-dimensional vector of correlation parameters $\bar{\theta} = \{\theta_1, \dots, \theta_n\}^T$. As mentioned above, by default Dakota determines the value of $\bar{\theta}$ using a Maximum Likelihood Estimation (MLE) procedure [4].

Another characteristic that makes RSM particularly suitable for the problem under examination is that GP has a hyper-parametric error model, so it can be used to model surfaces with slope discontinuities (see surface grids from DoEs at paragraph 2) along with multiple local minima and maxima.

In the case in question, the DoE provides a file in table form (*'table_out.dat'*) of 121 data rows and it was decided to apply the surrogate model by reading only in the points already available, not carrying out a resampling (which requires to call back the external solver Fluent). It is necessary to format the tabular file in such a way that it is correctly readable from Dakota input file; the formatted file has been denoted *'database.dat'* and referred to as *'samples_file'* in the surrogate model section of Dakota input file.

It is possible to print each of the populations generated by the genetic algorithm through *'print_each_pop'* command.

Final results from MOGA applied on the response surfaces have been output to a file called *'finaldata1.dat'* located inside the directory in which Dakota has been run.

3.1 MOGA on multidimensional parameter study DoE

The RSM (Kriging) has been initially applied to the DoE obtained from the multidimensional parameter study; the use of MOGA on the surrogate model lead to the following results:

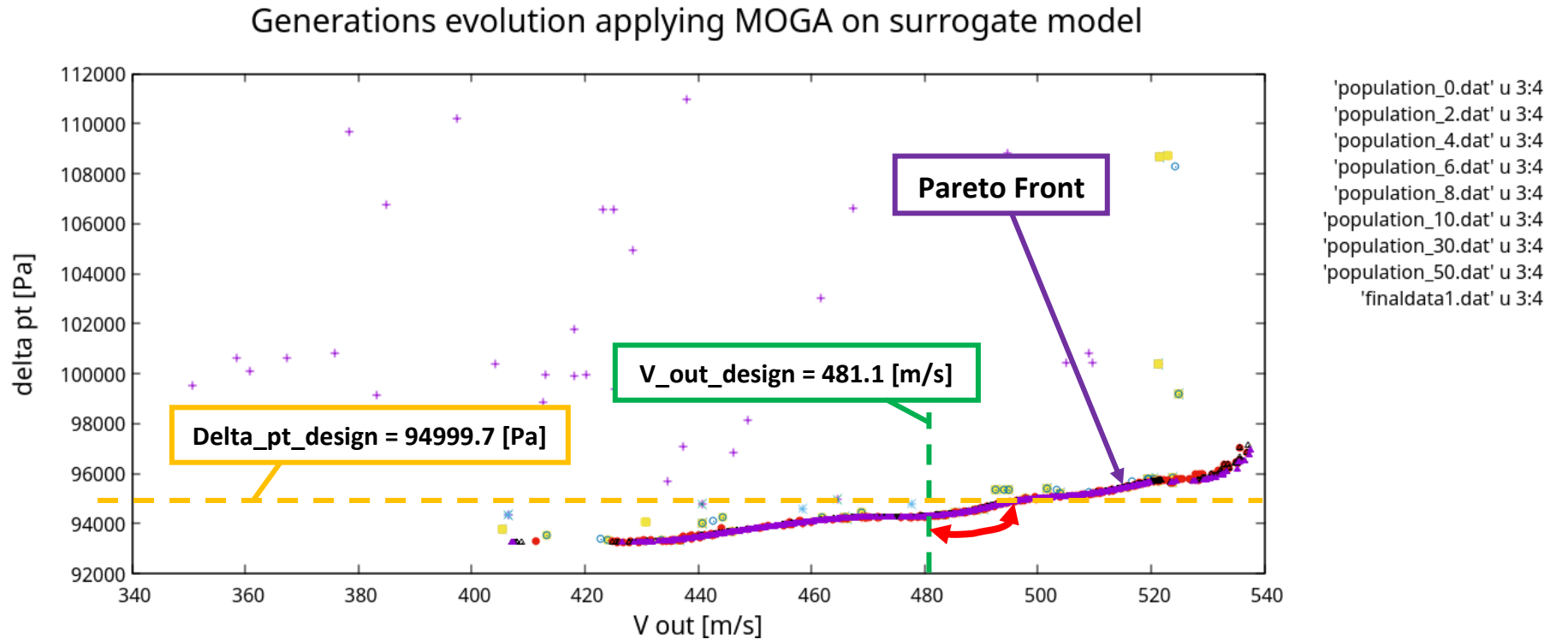


Figure 10 : plot of some generations ('populations') calculated by the genetic algorithm. The 'finaldata1.dat' series identifies the Pareto front of the problem

Moving from one generation ('population') of individuals to the next one, the MOGA gradually identifies a Pareto front of optimal solutions (purple triangles in Figure 10) within the parameter space made available to the optimizer ($T_{t1} = 300 \div 500$ [K] and $p_{t1} = 4 \div 6$ [bar]). Confirming the correct setting of the genetic algorithm, it is possible to note that already from the 30th generation ('population_30.dat' - red dots series), almost all the individuals selected by the GA fall on the aforementioned front.

Considering the set of “non-dominated” solutions (figure 10):

- the Pareto front includes cases whose divergent outlet flow speed is lower than 481.1 [m/s] (design point simulation - dotted green line), however these individuals show total pressure losses lower than design point value (94999.7 [Pa] – dotted yellow line);
- the remaining part of the Pareto includes solutions with an higher V_{out} than the design case, even if only a limited portion of them generates total pressure drops lower than the design point (region signed by red double arrow).

The performed optimization has therefore identified a set of solutions with divergent outlet flow speed higher and total pressure drop through the nozzle lower than the design point.

Input parameters combination evolution applying MOGA on surrogate model

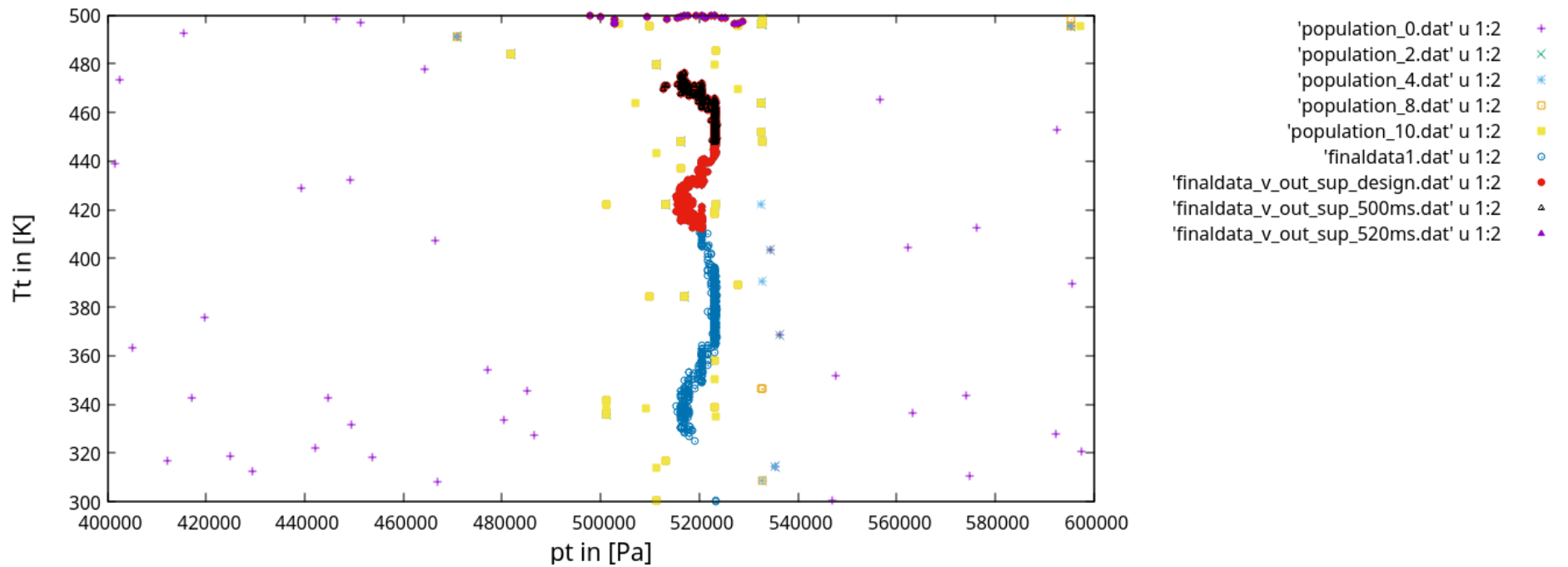


Figure 11 : distributions of points deriving from various combinations of input parameters operated by the genetic algorithm

From figure 11 it is interesting to note that:

- points belonging to the Pareto front ('finaldata1.dat' series - blue circles) are concentrated around the design point p_{t1} ($5\div 5.3$ [bar]);
- solutions with divergent outlet flow speed superior to the design point (red dots series) correspond to points with an inlet total pressure that does not exceed the design point value by more than 6%, while the total temperature seems to be much more incisive. In fact it is sufficient to note the different location in the parameter space of the “subsets” of final solutions: $V_{out} > 500$ [m/s] (black triangles series) with $T_{t1} = 450\div 480$ [K] and $V_{out} > 520$ [m/s] (purple triangles series) with $T_{t1} \approx 500$ [K], upper limit of the parameters space.

3.2 MOGA on LHS DoE

MOGA has been subsequently applied to the response surfaces generated from LHS DoE, leading to the following results:

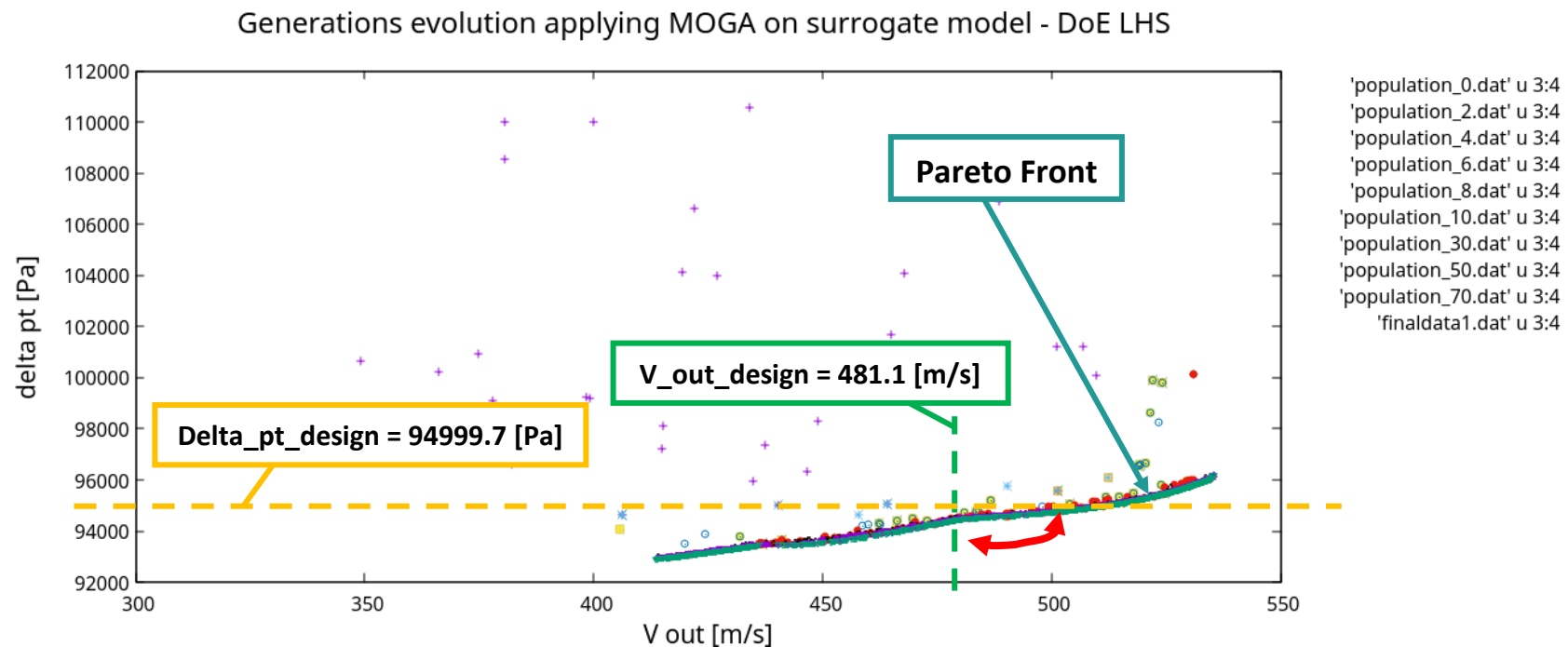


Figure 12 : plot of some generations ('populations') calculated by the genetic algorithm (DoE LHS). The 'finaldata1.dat' series identifies the Pareto front of the problem

Input parameters combination evolution applying MOGA on surrogate model - DoE LHS

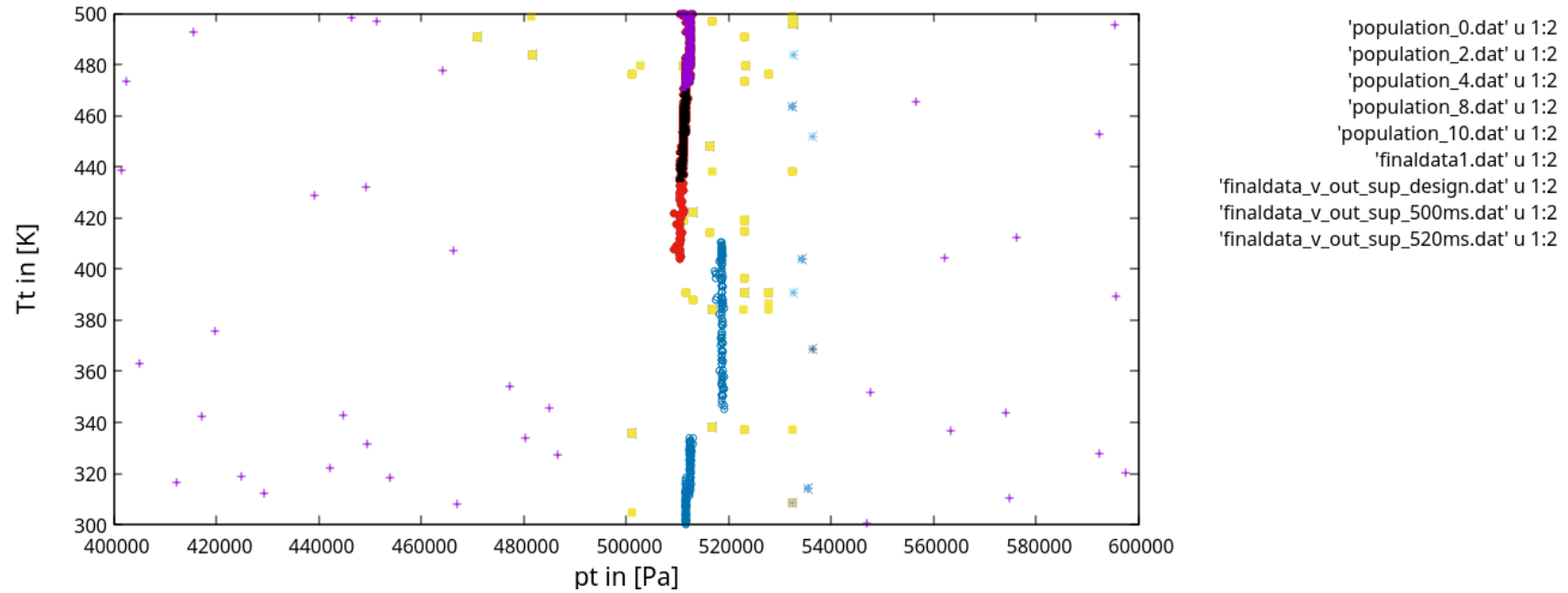


Figure 13 : distributions of points deriving from the various combinations of input parameters operated by the genetic algorithm (DoE LHS)

Even passing through a different DoE, the same Pareto front “shape” and location (in the design space) already seen in paragraph 3.1 have been reached. Input variables combinations in the parameter space lead to the same conclusions yet presented before at paragraph 3.1; it is possible to notice a lower variability of the total pressure (p_{t1}) in the set of solutions with nozzle outlet flow velocity higher than the design condition.

4. VALIDATION OF THE RESULTS OBTAINED BY APPLYING THE MOGA ON THE RS BUILT ON THE MULTIDIMENSIONAL PARAMETER STUDY DOE

In order to test the goodness of the generated meta-model and validate the results obtained, three “checking” CFD simulations have been conducted into three different “optima” of the Pareto displayed in figure 10:

- 1) maximum outlet flow speed from the divergent;
- 2) a solution that, compared to the design point, improves divergent outlet flow speed, reducing convergent-divergent crossing losses;
- 3) minimum total pressure drop across the nozzle.

MOGA+SBO CFD VALIDATION								
	BCs		MOGA ON RS		CFD		diff % MOGA-CFD	
	pt_in [Pa]	Tt_in [K]	V_out [m/s]	delta_pt [Pa]	V_out [m/s]	delta_pt [Pa]	V_out	delta_pt
Point 1	497821.3	500.0	537.6	96953.3	537.7	96943.3	-0.02%	0.01%
Point 2	516930.6	426.3	491.2	94647.8	491.2	94860.9	0.01%	-0.22%
Point 3	519052.2	324.8	426.6	93250.2	426.7	93037.9	-0.02%	0.23%

Table 4 : comparison between the results of the optimizer applied on the RS and the results of the CFD calculations

As shown in the results table above, the approximation obtained with the meta-model is very good, presenting maximum errors of about 0.2% on the prediction of the objective functions, but with a computational cost much lower than that required by applying the MOGA directly on the “true” physical model.

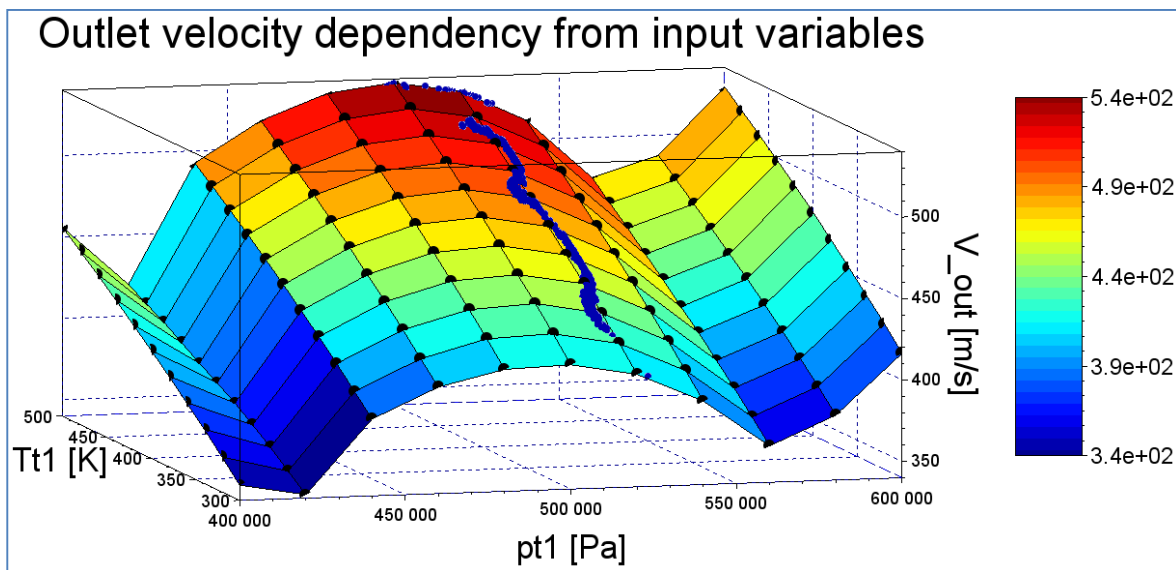


Figure 14 : scatter of Pareto front solutions (blue points) fall very close to divergent outlet flow speed surface plot

The last test on the goodness of the optimization carried out consists in plotting the final population identified by the genetic algorithm (*finaldata1.dat*) as a three-dimensional scatter around the objective function surfaces obtained by linear interpolation among the points of the DoE (see Figures 14 & 15). If the “individuals” of the final population are located very far from these surfaces, it is probable that the response surface method does not correctly approximate the physical model under examination and therefore the results of the optimization are not valid.

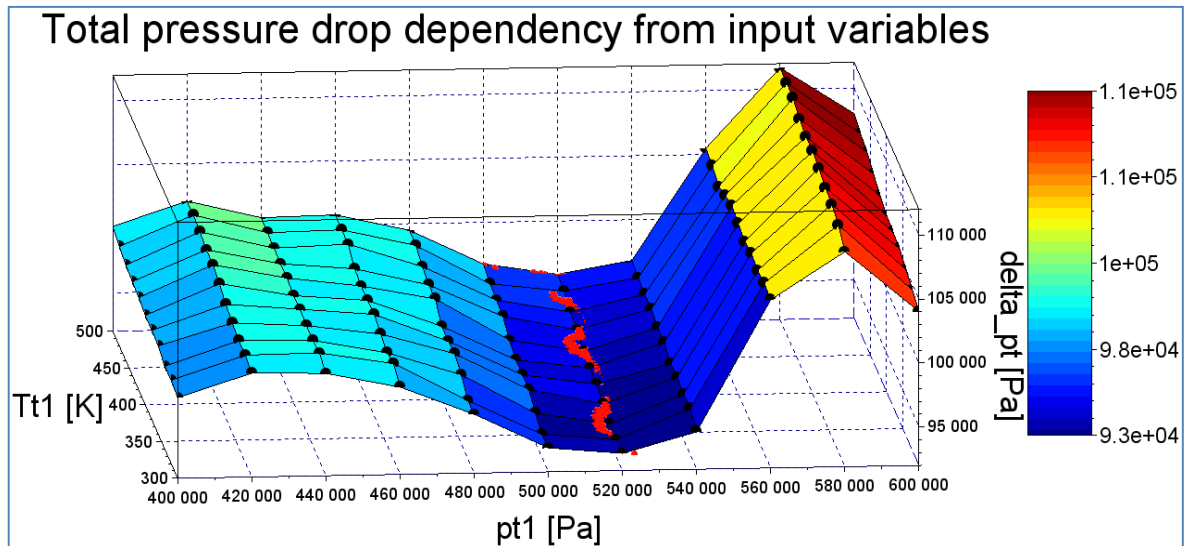


Figure 15 : scatter of Pareto front solutions (pink points) fall very close to nozzle crossing losses surface plot

As can be clearly seen in the images above (figures 14 & 15), the final population (Pareto front) falls almost exactly on the surfaces obtained by linear interpolation from the results of the DoE, identifying the maximum for divergent outlet flow speed and the minimum for the total pressure drop through the nozzle. These evidences confirm the validity of the results shown at paragraph 3.

CONCLUSIONS

The results achieved by the optimization process are in perfect agreement with the constraints of the problem and the laws of gas dynamics, in fact:

- a lowering of p_{t1} with respect to the design point is excluded from the MOGA as it would physically result in a raise of the ratio p_2/p_{t1} (p_2 is fixed at 120 [kPa]) i.e. shock wave in a section located even further upstream in the divergent [1, 2];
- an increase of p_{t1} with fixed geometry (and therefore throat section) would cause higher flow density, with consequent raise in nozzle permeability and therefore in total pressure losses through the duct (shock wave in any case located in the divergent due to the imposition of an outlet static pressure equal to the discharge pressure [1]);

- a raise in total temperature keeping the p_{t1} almost fixed allows to slightly widen the fluid dynamic throat section: the mass flow remains about the same of the design because the geometric throat is locked, so total pressure losses are limited, maximizing the flow velocity.

In conclusion, the condition that optimizes the performance of the nozzle is undoubtedly that in which the inlet total pressure remains substantially unchanged compared to the design point, in order to avoid an useless increase in entropy production, while inlet total temperature is raised, ensuring a decrease in flow density and therefore, with the geometric sections and mass flow locked, an increase in divergent outlet flow speed.

REFERENCES

[1] Ubaldi M., Academic year 2014/2015, Lecture notes of “Gasdynamics” course, Genoa University – Polytechnic School

[2] Anderson J. D., 1990, Modern compressible flow, McGraw-Hill

[3] Cravero C., Academic year 2015/2016, Lecture notes of “Numerical methods for fluid machinery and energy systems” course, Genoa University – Polytechnic School

[4] B. M. Adams, W. J. Bohnhoff, K. R. Dalbey, J. P. Eddy, M. S. Ebeida, M. S. Eldred, J. R. Frye, G. Gerarci, R. W. Hooper, P. D. Hough, K. T. Hu, J. D. Jakeman, M. Khalil, K. A. Maupin, J. A. Monschke, E. M. Ridgway, A. Rushdi, J. A. Stephens, L. P. Swiler, J. G. Winokur, D. M. Vigil, and T. M. Wildey. Dakota, a multilevel parallel object-oriented framework for design optimization, parameter estimation, uncertainty quantification, and sensitivity analysis: Version 6.8 user’s manual. Technical Report SAND2014-4633, Sandia National Laboratories, Albuquerque, NM, Updated May 2018

[5] Pralits J.O., Academic year 2017/2018, Lecture slides of “Optimal design in fluid dynamics” course, Genoa University – Polytechnic School

[6] Guerrero J., Academic year 2017/2018, Lecture notes of “Optimal design in fluid dynamics” course, Genoa University – Polytechnic School